molecular pharmaceutics

articles

Monitoring the Biodegradation of Dendritic Near-Infrared Nanoprobes by *in Vivo* Fluorescence Imaging

Adah Almutairi,[†] Walter J. Akers,[‡] Mikhail Y. Berezin,[‡] Samuel Achilefu,*[,‡] and Jean M. J. Fréchet*[,†]

College of Chemistry, University of California, Berkeley, California 94720-1460, and Department of Radiology, School of Medicine, Washington University, St. Louis, Missouri 63110

Received July 18, 2008; Revised Manuscript Received September 18, 2008; Accepted September 23, 2008

Abstract: Synthetic polymers and dendrimers have been widely used by the medical community to overcome biological barriers and enhance *in vivo* biomedical applications. Despite the widespread use of biomaterials it has been generally extremely difficult to monitor noninvasively their fate *in vivo*. Here we report multilayered nanoprobes, consisting of a near-infrared core, nanoencapsulated in a biodegradable dendrimer, and surrounded by a shell of polyethylene oxide. Covalent encapsulation of the near-infrared fluorophores in the dendritic scaffold conferred enhanced stability to the nanoprobe with added resistance to enzymatic oxidation and prolonged blood residence time. Insight into the time course of biodegradation of the dendritic aliphatic polyester nanoprobe was gained using noninvasive whole body *in vivo* fluorescence lifetime imaging. As the dendritic shell biodegrades the NIR probe becomes exposed, enabling monitoring of fluorescence lifetime changes *in vivo*.

Keywords: Near-infrared fluorescence imaging; whole body; fluorescence lifetime imaging; polymer biodegradation; biodistribution; dendrimer

Introduction

Over the past decade, the medical community has made widespread use of synthetic polymers and dendrimers to overcome complex biological barriers and enhance *in vivo* imaging,[1,2] drug delivery,[3] gene therapy[4] and tissue engineering.[5] Dendrimers are highly branched macromolecules that have a structural precision approaching that of proteins;[6,7] their globular structure provides a specific nanoenvironment

* To whom correspondence may be addressed. J.M.J.F.: College of Chemistry, University of California, 718 Latimer Hall, Berkeley, CA 94720-1460; tel, (510) 643-3077; fax, (510) 643-3079; e-mail, frechet@berkeley.edu. S.A.: Department of Radiology, School of Medicine, Washington University in St. Louis, St. Louis, MO 63110; tel, (314) 362-8599; e-mail, achilefus@mir.wustl.edu.

[†] University of California.

[‡] Washington University.

(1) Wiener, E. C.; Brechbiel, M. W.; Brothers, H.; Magin, R. L.; Gansow, O. A.; Tomalia, D. A.; Lauterbur, P. C. Dendrimer-Based Metal-Chelates - a New Class of Magnetic-Resonance-Imaging Contrast Agents. *Magn. Reson. Med.* **1994**, *31* (1), 1–8.

(2) Weissleder, R.; Tung, C. H.; Mahmood, U.; Bogdanov, A. In vivo imaging of tumors with protease-activated near-infrared fluorescent probes. *Nat. Biotechnol.* **1999**, *17* (4), 375–378.

(3) Lee, C. C.; Gillies, E. R.; Fox, M. E.; Guillaudeu, S. J.; Fréchet, J. M. J.; Dy, E. E.; Szoka, F. C. A single dose of doxorubicin-functionalized bow-tie dendrimer cures mice bearing C-26 colon carcinomas. *Proc. Natl. Acad. Sci. U.S.A.* **2006**, *103* (45), 16649–16654.

(4) KukowskaLatallo, J. F.; Bielinska, A. U.; Johnson, J.; Spindler, R.; Tomalia, D. A.; Baker, J. R. Efficient transfer of genetic material into mammalian cells using Starburst polyamidoamine dendrimers. *Proc. Natl. Acad. Sci. U.S.A.* **1996**, *93* (10), 4897–4902.

(5) Langer, R.; Vacanti, J. P. Tissue Engineering. *Science* **1993**, *260* (5110), 920–926.

(6) Tomalia, D. A.; Naylor, A. M.; Goddard, W. A. Starburst Dendrimers - Molecular-Level Control of Size, Shape, Surface-Chemistry, Topology, and Flexibility from Atoms to Macroscopic Matter. *Angew.Chem., Int. Ed. Engl.* **1990**, *29* (2), 138–175.

(7) Fréchet, J. M. J. Functional Polymers and Dendrimers - Reactivity, Molecular Architecture, and Interfacial Energy. *Science* **1994**, *263* (5154), 1710–1715.

10.1021/mp8000952 CCC: $40.75
Published on Web 10/21/2008

that surrounds a functional core thereby affecting its molecular properties.[8] The structural features and multivalency of dendrimers translate especially well into pharmacology, and have led to great promise in drug delivery.[9] Aliphatic polyester dendrimers based on the monomer 2,2-bis(hydroxymethyl)propanoic acid (bis-HMPA)[10−12] have low toxicity, low immunogenicity, and a biodegradable structure that makes them especially appealing for applications in biotechnology.[13,14] We envisioned that *labeled* dendrimers might well be suitable for the noninvasive reporting of the *in vivo* degradation of this class of aliphatic polyester dendrimers. Radioactive tracers are commonly attached to pharmaceuticals to monitor their biodistribution and elimination after injection. A potential limitation of this strategy is that the radiotracer can become separated from the molecule of interest at any time after injection. This separation cannot be detected through noninvasive means. The same is true for optically active (fluorescent) contrast agents in general when using near-infrared (NIR) fluorescence intensity for detection. Near-infrared light can pass through the skin, without damaging tissue, and with minimal absorption by water, hemoglobin, oxygenated hemoglobin, fat, and melanin.[15,16] Additionally, fluorescence from intrinsic tissue components (autofluorescence) is low in the NIR region, resulting in higher signal to background ratios.[16] The use of fluorescence lifetime in cellular and molecular biology, and in single molecule spectroscopy is rapidly expanding, because it utilizes the environmentally sensitive characteristics of excited-state decay. Therefore, the excited states of certain NIR fluorophores are greatly influenced by their local environment,[17] while remaining independent of the factors that impact fluorescence intensity imaging such as photobleaching and light path length.[18] Fluorescence lifetime measurements have been used to provide access to functional information on biomolecules,[19,20] tissue microenvironments,[18,21] and, to a much lesser extent, on living animals.[22−24] We hypothesized that fluorescence lifetime imaging (FLI) of the fluorescent reporter encapsulated within a dendritic nanoparticle would enable the noninvasive *in vivo* monitoring of the degradation of nanoparticle itself.

Herein, we describe the preparation of biodegradable aliphatic polyester dendritic nanoprobes decorated with a shell of polyethylene oxide (PEO) and a core consisting of a NIR fluorophore. We used whole body *in vivo* FLI to shed light on the biodegradation of these dendritic NIR nanoprobes. Changes in the decay characteristics of the fluorescent reporter without alteration of the fluorescence intensity enabled us to monitor the progressive biodegradation of the nanoprobes as well as their elimination from the body, a feat not currently possible with radioactive tracers.

Results and Discussion

We use the core of a third generation polyester dendrimer, possessing eight orthogonally protected branching sites, to covalently nanoencapsulate cypate,[25] a polymethine dye

(8) Hecht, S.; Fréchet, J. M. J. Dendritic encapsulation of function: Applying nature's site isolation principle from biomimetics to materials science. *Angew. Chem., Int. Ed.* **2001**, *40* (1), 74–91.
(9) Lee, C. C.; MacKay, J. A.; Fréchet, J. M. J.; Szoka, F. C. Designing dendrimers for biological applications. *Nat. Biotechnol.* **2005**, *23* (12), 1517–1526.
(10) Ihre, H.; Hult, A.; Soderlind, E. Synthesis, characterization, and H-1 NMR self-diffusion studies of dendritic aliphatic polyesters based on 2,2-bis(hydroxymethyl)propionic acid and 1,1,1-tris(hydroxyphenyl)ethane. *J. Am. Chem. Soc.* **1996**, *118* (27), 6388–6395.
(11) Ihre, H.; De Jesus, O. L. P.; Fréchet, J. M. J. Fast and convenient divergent synthesis of aliphatic ester dendrimers by anhydride coupling. *J. Am. Chem. Soc.* **2001**, *123* (25), 5908–5917.
(12) Ihre, H. R.; De Jesus, O. L. P.; Szoka, F. C.; Fréchet, J. M. J. Polyester dendritic systems for drug delivery applications: Design, synthesis, and characterization. *Bioconjugate Chem.* **2002**, *13* (3), 443–452.
(13) De Jesus, O. L. P.; Ihre, H. R.; Gagne, L.; Frechet, J. M. J.; Szoka, F. C. Polyester dendritic systems for drug delivery applications: In vitro and in vivo evaluation. *Bioconjugate Chem.* **2002**, *13* (3), 453–461.
(14) Gillies, E. R.; Dy, E.; Fréchet, J. M. J.; Szoka, F. C. Biological Evaluation of Polyester Dendrimer: Poly(ethylene oxide) "Bow-Tie" Hybrids with Tunable Molecular Weight and Architecture. *Mol. Pharmaceutics* **2005**, *2* (2), 129–138.
(15) Rudin, M.; Weissleder, R. Molecular imaging in drug discovery and development. *Nat. Rev. Drug Discovery* **2003**, *2* (2), 123–131.
(16) Sevick-Muraca, E. M.; Houston, J. P.; Gurfinkel, M. Fluorescence-enhanced, near infrared diagnostic imaging with contrast agents. *Curr. Opin. Chem. Biol.* **2002**, *6* (5), 642–650.
(17) Berezin, M. Y.; Lee, H.; Akers, W.; Achilefu, S. Near infrared dyes as lifetime solvatochromic probes for micropolarity measurements of biological systems. *Biophys. J.* **2007**, *93* (8), 2892–2899.
(18) Gadella, T. W. J.; Jovin, T. M.; Clegg, R. M. Fluorescence Lifetime Imaging Microscopy (Flim) - Spatial-Resolution of Microstructures on the Nanosecond Time-Scale. *Biophys. Chem.* **1993**, *48* (2), 221–239.
(19) Berezin, M. Y.; Lee, H.; Akers, W.; Nikiforovich, G.; Achilefu, S. Ratiometric analysis of fluorescence lifetime for probing binding sites in albumin with near-infrared fluorescent molecular probes. *Photochem. Photobiol.* **2007**, *83* (6), 1371–1378.
(20) Yang, H.; Luo, G. B.; Karnchanaphanurach, P.; Louie, T. M.; Rech, I.; Cova, S.; Xun, L. Y.; Xie, X. S. Protein conformational dynamics probed by single-molecule electron transfer. *Science* **2003**, *302* (5643), 262–266.
(21) Lakowicz, J. R.; Szmacinski, H.; Nowaczyk, K.; Berndt, K. W.; Johnson, M. Fluorescence Lifetime Imaging. *Anal. Biochem.* **1992**, *202* (2), 316–330.
(22) Bloch, S.; Lesage, F.; McIntosh, L.; Gandjbakhche, A.; Liang, K. X.; Achilefu, S. Whole-body fluorescence lifetime imaging of a tumor-targeted near-infrared molecular probe in mice. *J. Biomed. Opt.* **2005**, *10* (5), 0540031−0540038.
(23) Cubeddu, R.; Comelli, D.; D'Andrea, C.; Taroni, P.; Valentini, G. Time-resolved fluorescence imaging in biology and medicine. *J.Phys. D: Appl.Phys.* **2002**, *35* (9), R61−R76.
(24) Reynolds, J. S.; Troy, T. L.; Mayer, R. H.; Thompson, A. B.; Waters, D. J.; Cornell, K. K.; Snyder, P. W.; Sevick-Muraca, E. M. Imaging of spontaneous canine mammary tumors using fluorescent contrast agents. *Photochem. Photobiol.* **1999**, *70* (1), 87–94.
(25) Achilefu, S.; Dorshow, R. B.; Bugaj, J. E.; Rajagopalan, R. Novel receptor-targeted fluorescent contrast agents for in vivo tumor imaging. *Invest. Radiol.* **2000**, *35* (8), 479–485.

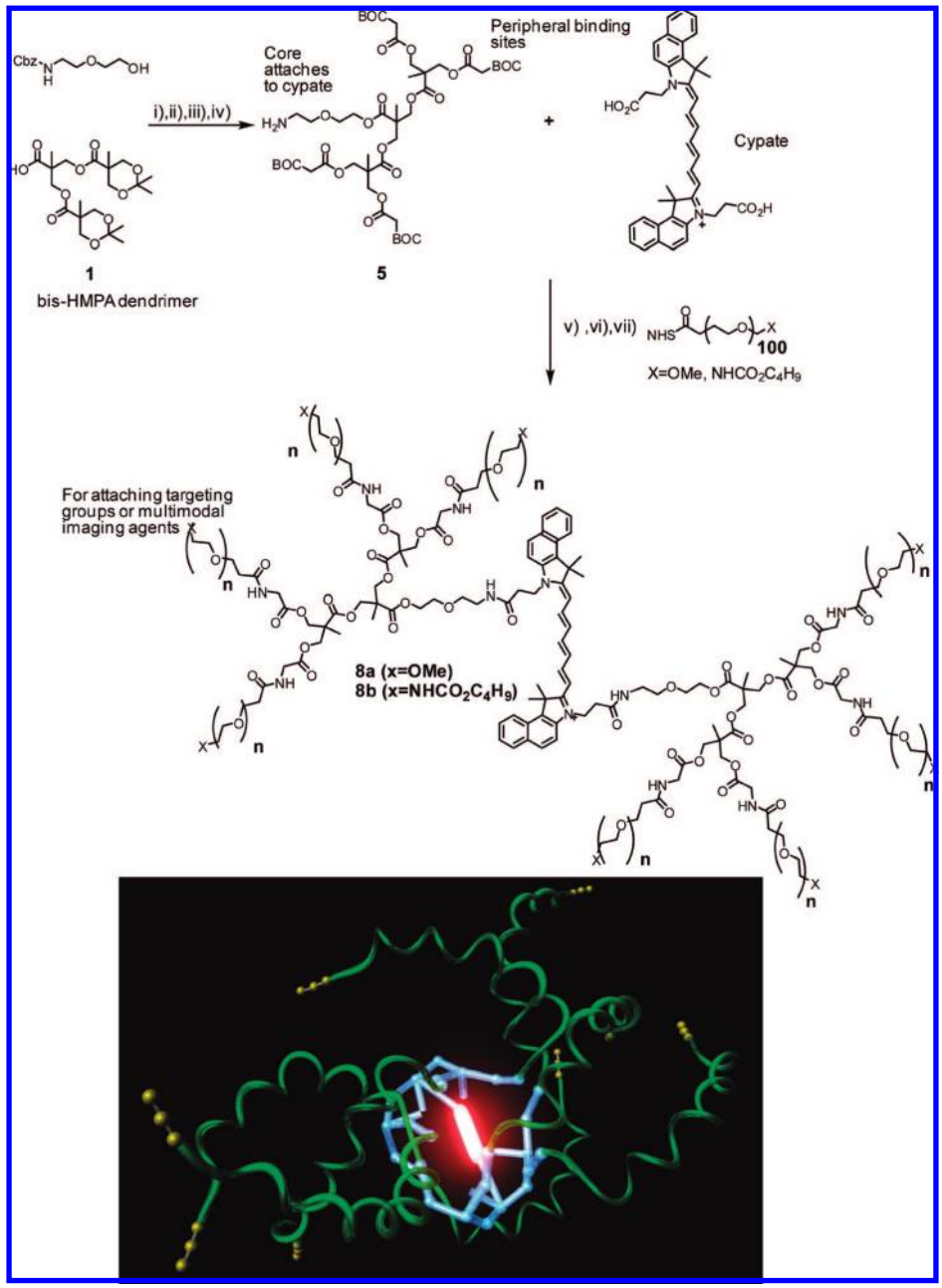

Figure 1. Preparation of nanoencapsulated near-infrared imaging agents. (i) DCC, DPTS, CH_2Cl_2, 91%, (ii) DOWEX acidic resin, MeOH, 99%, (iii) BOC-Gly, EDC, DMAP, DMF, 93%, (iv) Pd/C, H_2, THF, 18 h 98%, (v) EDC, HOBt, DMF, 0 °C, 78%, (vi) TFA, CH_2Cl_2, 0 °C, (vii) DMF, NEt_3, 100%.

related to indocyanine green (ICG), an FDA approved contrast agent for optical imaging. Cypate is capable of absorption and emission in the narrow tissue transparency window (750−850 nm), and has been functionalized with high affinity peptides[26] and applied to optical molecular imaging of living animals.[22,27] The cypate was encapsulated in a biodegradable polyester[9] dendrimer to both dictate fluorescence lifetime properties and prevent its aggregation (see Figure 1 for the synthetic scheme). The peripheral binding sites of the dendrimer were then used to graft eight polyethylene oxide (PEO) chains that are known to impart biological stealth and modulate blood retention.[14] Indeed, the resulting nanoprobe, with a molecular weight of *ca.* 40,000 Da and a polydispersity index of 1.02, had a

(26) Achilefu, S.; Bloch, S.; Markiewicz, M. A.; Zhong, T. X.; Ye, Y. P.; Dorshow, R. B.; Chance, B.; Liang, K. X. Synergistic effects of light-emitting probes and peptides for targeting and monitoring integrin expression. *Proc. Natl. Acad. Sci. U.S.A.* **2005**, *102* (22), 7976–7981.

(27) Achilefu, S. Lighting up tumors with receptor-specific optical molecular probes. *Techno. Cancer Res. Treat.* **2004**, *3* (4), 393–409.

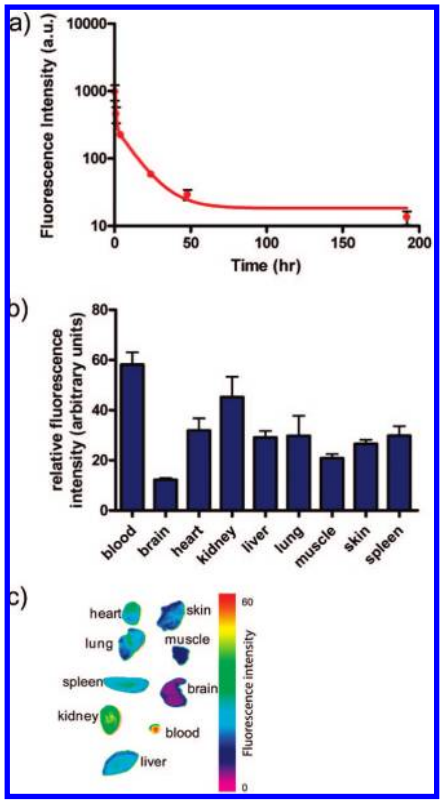

Figure 2. (a) Pharmacokinetic analysis of clearance of NIR stealth nanoprobes from the blood of mice. A two-compartment model was fit to the blood fluorescence data. Elimination half-life was determined to be 8.67 h by two phase exponential decay model. (b) *Ex vivo* fluorescence biodistribution assay 24 h p.i. High fluorescence signal was still observed in blood at this time-point, with relatively low accumulation in the liver and spleen. (c) The tissue residence time as measured by *ex vivo* fluorescence tissue biodistribution in blood, kidney, liver and muscle tissues.

prolonged plasma circulation time of nine hours (Figure 2a) as compared to less than five minutes for ICG.[28,29] Such blood circulation times are suitable for cardiovascular and blood pool imaging.[30] Furthermore, accumulation of the nanoprobes in normal tissues, besides the blood, was low (Figure 2c). However, preliminary results indicate passive accumulation in traumatized tissue (for details please see

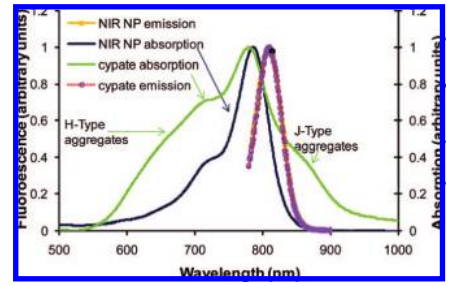

Figure 3. Steady state absorption and emission properties of the infrared imaging agent cypate and the NIR nanoprobes. In buffered aqueous solutions (10% MeOH), cypate may form H type aggregates, while the NIR nanoprobes show diminished aggregation in all the buffers, and organic solutions we tried.

Materials and Methods and SI Figure 3 in the Supporting Information). This is in agreement with data from similar systems that passively target diseased tissue susceptible to the enhanced permeation and retention (EPR) effect observed in tissue injury and many types of cancer.[31] No toxic effects, including abnormal behavior or weight loss/gain, were observed during an eight-day observation period after mice were injected with 1 mg (40 mg/kg) of the biodegradable stealth NIR dendritic nanoprobe.

These NIR dendritic nanoprobes offer a favorable pharmacokinetic profile for multivalent ligand presentation. The biological stealth properties imparted by the PEO chains allow the nanoprobes to efficiently evade the reticuloendothelial system (RES) for more than 24 h after injection, leaving a significant circulating concentration. Low accumulation in healthy tissue bodes well for targeting efforts. To this end we have successfully synthesized NIR dendritic nanoprobes with heterobifunctional PEO chains (Figure 1) that are amenable to labeling with ligands at the terminal ends of the PEO chains for multivalent targeting of desired tissue.

The steady state absorption and emission of these NIR dendritic nanoprobes in buffers showed substantially less aggregation than observed with cypate (Figure 3). Molar absorptivities remained similar and the quantum efficiencies of cypate and the NIR dendritic nanoprobes were found to be 2% and 4%, respectively, in water. However, major differences were observed in dynamic fluorescent behavior. Specifically the relaxation rate of the NIR dendritic nanoprobe was unaffected by opsonization remaining monoexponential at 0.3 ns (ns), even in the presence of albumin, a ubiquitous serum protein. On the other hand the lifetime of cypate changes from a monoexponential lifetime of 0.2 ns in aqueous solutions, to a bis-exponential decay of lifetimes at 0.47 ns, and 0.97 ns in the presence of albumin. The lifetime of the NIR dendritic nanoprobes also remains constant in solvents such as dimethyl sulfoxide (DMSO) and

(28) Cuccia, D. J.; Bevilacqua, F.; Durkin, A. J.; Merritt, S.; Tromberg, B. J.; Gulsen, G.; Yu, H.; Wang, J.; Nalcioglu, O. In vivo quantification of optical contrast agent dynamics in rat tumors by use of diffuse optical spectroscopy with magnetic resonance imaging coregistration. *Appl. Opt.* **2003**, *42* (16), 2940–2950.

(29) Gurfinkel, M.; Thompson, A. B.; Ralston, W.; Troy, T. L.; Moore, A. L.; Moore, T. A.; Gust, J. D.; Tatman, D.; Reynolds, J. S.; Muggenburg, B.; Nikula, K.; Pandey, R.; Mayer, R. H.; Hawrysz, D. J.; Sevick-Muraca, E. M. Pharmacokinetics of ICG and HPPH-car for the detection of normal and tumor tissue using fluorescence, near-infrared reflectance imaging: A case study. *Photochem. Photobiol.* **2000**, *72* (1), 94–102.

(30) Jaffer, F. A.; Weissleder, R. Seeing within - Molecular imaging of the cardiovascular system. *Circ. Res.* **2004**, *94* (4), 433–445.

(31) Matsumura, Y.; Maeda, H. A New Concept for Macromolecular Therapeutics in Cancer-Chemotherapy - Mechanism of Tumoritropic Accumulation of Proteins and the Antitumor Agent Smancs. *Cancer Res.* **1986**, *46* (12), 6387–6392.

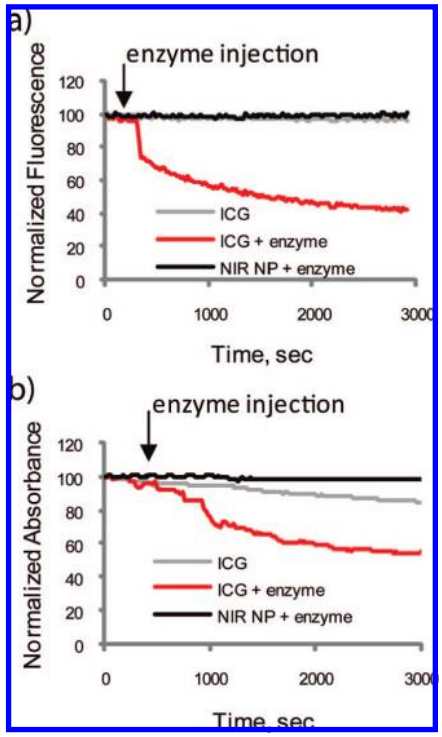

Figure 4. ICG was found to be moderately stable to degradation within one hour in pure water, indicated by an almost horizontal line. (a) After the addition of microsomes and NADPH regenerating systems, the emission of ICG immediately dropped by 30% and continued declining within the experimental time frame. The absorption kinetics curve (b) closely matched the emission data indicating the loss of the ICG's polymethine chromophore and not the emission quenching. The destruction of the chromophore apparently proceeds via an oxidation pathway and is catalyzed by cytochrome P450, a metabolic enzyme in liver microsomes. In contrast, the NIR dendritic nanoprobes are much more stable toward enzymatic oxidation, likely due to the protective layer around the chromophore.

dichloromethane, while the lifetime of cypate increases to 0.9 ns of monoexponential decay in DMSO, a more hydrophobic environment better capable of stabilizing its excited state.

Furthermore, we observed a significant difference in stability to enzymatic degradation between free indocyanine green (ICG) and our NIR dendritic nanoprobe. We tested ICG instead of cypate because cypate tends to agglomerate on the hydrophobic membrane of the microsomes used in this study. ICG was found to be moderately stable to degradation within one hour in pure water, as indicated by an almost horizontal emission line (Figure 4a). After the addition of microsomes and NADPH regenerating systems, the emission of ICG immediately dropped by 30% and continued to decline through the time frame of the experiment. The absorption kinetics curve (Figure. 4b) closely matches the emission data in Figure 4a indicating the loss of the ICG's polymethine chromophore and not emission quenching. Destruction of the chromophore apparently

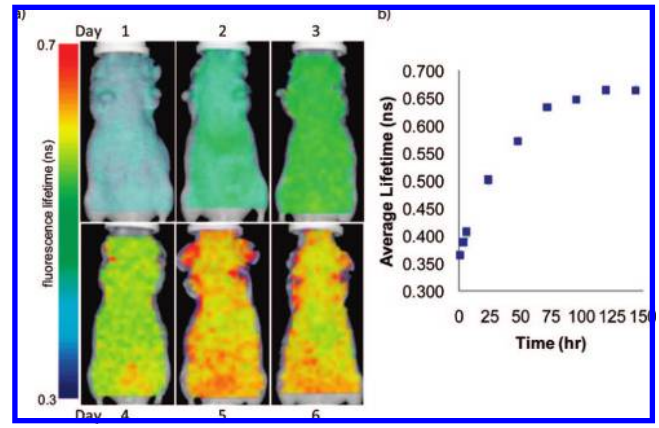

Figure 5. (a) Fluorescence lifetime maps of site-isolated NIR fluorescent nanoprobes *in vivo* at 1−6 days postinjection. The lifetimes detected are homogeneous for the first hour but gradually begin to increase heterogeneously in a site specific manner. Highest lifetimes are seen in the liver and intestines, likely due to increased metabolism of the nanoprobes. (b) A plot of average measured fluorescence lifetime as a function of time in the liver. The measured fluorescence lifetime *in vivo* increased over time with a significantly nonzero slope ($p < 0.01$) of 0.004 ns/h and intercept of 0.35 ns using a linear correlation model of 0−50 h.

proceeds via an oxidative pathway catalyzed by cytochrome P450, a metabolic enzyme in liver microsomes. In contrast to ICG, and as clearly seen in Figure 4, the NIR dendritic nanoprobes are much more stable toward enzymatic oxidation, due to the protective layer around the chromophore.

The biodegradable structure of the NIR dendritic nanoprobe can only offer this nanoenvironment independent of *in vivo* or *in vitro* factors until its metabolic erosion. Degradation studies on these aliphatic polyester dendrimers conducted in buffers (pH 5 and 7.4) have shown full degradation after three weeks.[14] There are few techniques for noninvasive *in vivo* monitoring of the biodegradation of biomaterials,[32] and to the best of our knowledge, none using optical methods. Herein we use FLI to monitor polymer degradation kinetics *in vivo*. Whole-body fluorescence lifetime maps, shown in Figure 5, were created from time-domain whole-body fluorescence imaging at indicated time points after injection of the nanoprobes. The NIR dendritic nanoprobes have relatively homogeneous fluorescence lifetime maps. In contrast, earlier *in vivo* fluorescence lifetime imaging (FLI) measurements with cypate yielded heterogeneous lifetime maps[22] ranging from 0.7−0.8 ns, with similarly heterogeneous intensity maps.[22] *In vivo* fluorescence lifetime changes over a seven day period allowed us to monitor the degradation kinetics of the dendritic nanoprobe in real time. No changes in the fluorescence lifetime images over time were observed when using cypate throughout the

(32) Mader, K.; Bacic, G.; Domb, A.; Elmalak, O.; Langer, R.; Swartz, H. M. Noninvasive in vivo monitoring of drug release and polymer erosion from biodegradable polymers by EPR spectroscopy and NMR imaging. *J. Pharm. Sci.* **1997**, *86* (1), 126–134.

duration of imaging.[22] We suspect the hydrolysis of this aliphatic dendrimer leads to exposure of the NIR fluorophore which is then rapidly opsonized. Opsonization of the NIR fluorophore leads to the change in fluorescent lifetime indicating the degradation of the dendritic nanoparticle.

Conclusion

In conclusion, we have found that three important advantages arise from incorporating cypate in a biodegradable dendritic scaffold: (i) Nanoprobe degradation kinetics can be monitored *in vivo* by the rate of fluorescence lifetime change, while the metabolic activity of tissue and its microenvironment is probed; (ii) immediate opsonization of the contrast agent and its degradation can be prevented; and (iii) accumulation in the RES can be significantly reduced to yield a long circulating NIR contrast nanoprobe useful as a blood pool and cardiovascular system imaging agent.

Examples of biodegradable NIR imaging agents capable of prolonged blood residence times, free of nonspecific accumulation in healthy tissue, are rare.[33] Our system can function as a universal carrier for active multivalent targeting with peptides, as well as for passive targeting of diseased tissue suffering from the EPR effect, seen in cancerous and inflamed tissue. The biodegradable nature of this NIR dendritic nanoprobe enables extraction of functional information through fluorescence lifetime changes. Furthermore, this layered approach can provide a means of sensing physiological differences by changes in the fluorescence lifetimes of NIR probes the biodegradation profile of the encapsulating biomaterial. NIR fluorescence lifetime changes as a function of time could provide valuable functional information on tissue physiology, metabolism, and protein binding[34] in a site-specific and tissue specific manner.

Materials and Methods

General Methods. All reagents were purchased from Sigma-Aldrich. and used as received except for the following: pyridine, dichloromethane (DCM), tetrahydrofuran (THF), and *N*,*N*-dimethylformamide (DMF) were purchased from Fisher and purified by passing them under nitrogen pressure through two packed columns (Glass Contour) of either neutral alumina (pyridine) or activated molecular sieves (DMF, DCM, THF). Nanopure grade water was used for all aqueous formulations. *N*,*N*-Dimethylaminopyridinium *p*-toluenesulfonate was prepared according to the literature. Dendrimer **1** was prepared as reported.[11] Monofunctional and heterobifunctional polyethylene oxide were purchased from Nektar. Cypate was prepared as previously reported.[25] All glassware was flame dried, evacuated of air and back filled with nitrogen gas unless otherwise noted. ^{1}H NMR spectra were recorded on a Bruker AVB-400 MHz instrument and all ^{13}C NMR spectra were recorded at 125 MHz. NMR chemical shifts are reported in parts per million (ppm) and coupling constants are reported in Hertz (Hz) and calibrated against $CDCl_3$ (δ 7.26, 77.00) or CD_2Cl_2-d_6 (δ 5.32) as indicated. Matrix assisted laser desorption ionization time-of-flight (MALDI-TOF) mass spectrometry experiments were performed on a PerSeptive Biosystems Voyager-DE from PerSeptive Biosystems using a nitrogen laser (337 nm). Samples were prepared by mixing dilute solutions (~0.1 mM) of the analyte in THF with approximately equal volumes of a 0.1 M solution of *trans*-3-indoleacrylic acid in THF, followed by deposition of 1 μL sample solution onto a 100-well gold plate and air drying. Extracts were dried over $MgSO_4$ and solvents were removed with a rotary evaporator at aspirator pressure. Chromatography was carried out with Merck silica gel for flash columns, 230−400 mesh. The solvents used for absorbance were spectroscopic grade. Size exclusion chromatography in DMF solution was carried out at 1.0 mL/min thermostatted at 35 °C. The SEC system consisted of a Waters 510 pump, a Waters 717 autosampler, a Waters 486 UV/vis detector, and a Wyatt Optilab differential refractive index detector.

Synthetic Protocols. A convergent synthetic approach was adopted due to the sensitive nature of the NIR dye.

Cbz-G2-acetonide Protected (2). Cbz-2-(2-hydroxy ethoxy)-ethylene amine (1 g, 9.6 mmol), dendrimer **1** (3.6 g, 8 mmol), and DPTS (47 mg, 1.6 mmol) were dissolved in DCM (50 mL), and then DCC (1.65 mg, 8 mmol) was added. After 4 h, the reaction was done (MALDI). It was diluted with DCM (200 mL) and washed with 1 M $NaHSO_4$ (3 × 100 mL), 1 M NaOH (3 × 100 mL), and water (2 × 100 mL). The organic layer was dried and filtered, and the solvent was removed under reduced pressure. The desired product was purified by column chromatography using a 3:2 hexanes:EtOAc solution as the mobile phase to yield a clear colorless oil (5.3 g, 91%). ^{1}H NMR (400 MHz, $CDCl_3$): δ ppm 1.13 (s, 6H), 1.27 (s, 3H), 1.34 (s, 6H), 1.40 (s, 6H), 3.36 (dd, J = 10.35, 5.22 Hz, 2H), 3.53 (t, J = 4.93, 4.93 Hz, 2H), 3.60 (s, 2H), 3.64 (m, 4H), 4.14 (d, J = 11.69 Hz, 4H), 4.24 (m, 2H), 4.31 (s 4H), 5.09 (s, 2H), 5.43 (bs, 1H), 7.34 (m, 5H). ^{13}C NMR (400 MHz, $CDCl_3$): 173.49, 128.45, 128.04, 98.11, 69.98, 68.58, 66.63, 65.91, 65.88, 65.30, 64.10, 46.78, 41.98, 24.99, 22.15, 18.53, 17.63. MALDI-TOF MS: $[M + Na]^+$ 692.7.

Cbz-G2-OH (3). Cbz-G2-acetonide protected (**2**) (264 mg, 180 mmol) was dissolved in methanol, a spatula full of Dowex acidic resin was added, and the reaction mixture was stirred overnight. Reaction gave a single clean product by MALDI; then filtration and concentration under reduced pressure yielded a clear colorless oil (233 mg, 99%). ^{1}H NMR (400 MHz, $CDCl_3$): δ ppm 1.04 (s, 6H), 1.30 (s, 3H), 3.37−3.39 (m, 2H), 3.55 (t, J = 4.90, 4.90 Hz, 2H), 3.67 (m, 2H), 3.76 (dd, J = 44.84, 11.50 Hz, 8H), 4.28 (m, 2.5H),

(33) Flaumenhaft, R.; Tanaka, E.; Graham, G. J.; De Grand, A. M.; Laurence, R. G.; Hoshino, K.; Hajjar, R. J.; Frangioni, J. V. Localization and quantification of platelet-rich thrombi in large blood vessels with near-infrared fluorescence Imaging. *Circulation* **2007**, *115* (1), 84–93.

(34) Almutairi, A.; Guillaudeu, S. J.; Berezin, M. Y.; Achilefu, S.; Frechet, J. M. J. Biodegradable pH-sensing dendritic nanoprobes for near-infrared fluorescence lifetime and intensity imaging. *J. Am. Chem. Soc.* **2008**, *130* (2), 444–445.

4.32 (s, 1H), 4.42 (d, $J = 11.15$ Hz, 2H), 5.10 (s, 2H), 5.57 (bs, 1H), 7.35 (m, 5H). MALDI-TOF MS: $[M + Na]^+$ 610.7.

Cbz-G2-BOC-Gly (4). Cbz-G2-OH (**3**) (74 mg, 0.126 mmol), Boc-Gly-OH (174 mg, 1.01 mmol), and DPTS (54 mg, 0.201 mmol) were dissolved in DMF (3 mL), then EDC (192 mg, 1.01 mmol) was added, and reaction mixture was stirred overnight. After 24 h, the reaction was done (MALDI, IAA). It was diluted with diethyl ether (35 mL) and washed with 1 M $NaHSO_4$ (3 × 25 mL), 1 M NaOH (3 × 25 mL), and water (2 × 25 mL). The organic layer was dried and filtered, and the solvent was removed under reduced pressure to yield a clear colorless oil (145 mg, 93%). ^{1}H NMR (400 MHz, $CDCl_3$): δ ppm 1.28 (s, 6H), 1.29 (s, 3H), 1.47 (s, 36H), 3.41 (dd, $J = 10.48$, 5.24 Hz, 2H), 3.59 (t, $J = 5.02$ Hz, 2H), 3.67 (m, 2H), 3.91 (d, $J = 5.71$ Hz, 8H) 4.29 (m, 14H), 5.13 (s, 2H), 5.53 (bs, 4H), 7.38 (m, 5H). ^{13}C NMR (400 MHz, $CDCl_3$): 155,643; 149,193; 128,391; 127,992; 52,118; 44,794; 44,607; 42,187; 38,967; 35,373; 28,243; 28,215; 14,633. MALDI-TOF MS: $[M + Na]^+$ 1238.3.

NH_2-G2-BOC-Gly (5). Cbz-G2-BOC-Gly (**4**) (130 mg, 0.105 mmol) was dissolved in dry THF (2 mL), 20 mg of a mixture of 10% palladium on activated carbon was added, and the mixture was pressurized under a hydrogen atmosphere, stirred overnight, and monitored by MALDI. The mixture was diluted with THF and then filtered through Celite. The combined filtrate was concentrated under reduced pressure to obtain **5** as a clear, colorless oil (114 mg, 98%). MALDI-TOF MS: $[M + Na]^+$ 1104.6.

Didendronized Cypate-BOC-Gly (6). Cypate (4 mg, 0.006 mmol) was dissolved in dry DMF (2 mL) and cooled to 0 °C, EDC was added (2.4 mg, 0.013 mmol), and the mixture was stirred for 5 min. HOBt (1.6 mg, 0.012 mmol) was added while stirring was maintained at 0 °C, and the mixture was left to react for 15 min. NH_2-G2-BOC-Gly (**5**) (20 mg, 0.019 mmol) was added, and the reaction was monitored by MALDI. After 2 h all the starting materials were consumed. The reaction was concentrated down and redissolved in DCM. The organic layer was washed with 1 M $NaHSO_4$ (3 × 15 mL), 1 M NaOH (3 x15 mL), and water (2 × 15 mL). The organic layer was dried and filtered, and the solvent was removed under reduced pressure. The desired product was purified by column chromatography using 9:1 DCM:MeOH as the mobile phase. The desired product was a dark green solid (12.8 mg, 78%) ^{1}H NMR (400 MHz, $CDCl_3$): δ ppm 1.22 (s, 6H), 1.25 (s, 3H), 1.42 (s, 36H), 1.77 (bs, 6H), 1.95 (s, 5H), 2.85 (m, 2H), 3.39 (m, 2H), 3.52 (m, 2H), 3.59 (m, 2H), 3.88 (d, $J = 5.73$ Hz, 8H), 4.24 (m, 14H), 4.49 (m, 2H), 5.52 (bs, 4H), 6.51 (d, $J = 11.86$ Hz, 2H), 6.77 (m, 2H), 7.40−7.47 (m, 2H), 7.56−7.62 (m, 3H), 7.77−7.84 (m, 2H), 7.92−8.09 (m, 7H). MALDI-TOF MS: [M] 2749.6.

General Procedure for Grafting Polyethylene Chains on to the Dendrimers. Didendronized PEGylated Cypate (8a). Didendronized Cypate-Gly (7). A 4:1 mixture of dry DCM and TFA (2 mL) was cooled to 0 °C and used to dissolve didendronized cypate-BOC-Gly (**6**) (25 mg, 0.009 mmol). The solution immediately turned purple and then biphasic. The reaction was monitored by MALDI and was complete after two hours of stirring. The solvents were removed under reduced pressure yielding a green solid, and taken to the next step without any further purification. MALDI-TOF MS: $[M]^+$ m/z 2068.4. Didendronized cypate-Gly (**7**) was redissolved in anhydrous toluene (2 mL), and NEt_3 (10 μL). To this mixture was added NHS-PEO_{5000}-BOC (400 mg, 0.076 mmol), and the mixture was vortexed to ensure proper mixing. The reaction was stirred for 36 h and monitored by SEC. A PEO standards calibration curve was established, and the predicted MW was 40,000 Da with a PDI of 1.02. Reaction was concentrated down, redissolved in nano pure water, and purified by ultrafiltration (membrane MWCO 50 kDa) to remove excess PEO chains. After freeze-drying, a fluffy white powder was recovered in 90% yield (324 mg). DMF SEC showed a peak around 40,000 Da, PDI 1.02, and another at 5000 Da corresponding to the excess PEO (>1%) (see Supporting Information). Dynamic light scattering measurements were attempted on this nanoparticle to characterize its hydrodynamic volume, however, the core dye absorbed the laser light (650 nm) making it difficult to take these measurements. Nanoparticles with the same branching, chemical compositions, size exclusion chromatograms and molecular weight, were synthesized without the NIR dye and found their hydrodynamic diameters to be in the range of 7−10 nm (see Supporting Information).

Steady State Absorption, Fluorescence Emission, and Lifetime Measurements. Ground state UV/vis/NIR absorption spectra were measured on either a Cary 50 UV−vis spectrophotometer or a Shimadzu UV−vis-NIR spectrophotometer. Samples for absorbance and emission experiments were measured in standard 1 cm quartz cells. All measurements were performed at room temperature.

Stabilities of ICG and the NIR dendritic nanoprobes were assessed by monitoring (i) absorption at 780 nm and (ii) emission at 820 nm with excitation at 780 nm. In both methods, the sampling was conducted every 20 s for one hour. Emission was monitored in antibleaching mode with constant stirring, the emission signal was corrected by lamp intensity (S/R). Experiments were conducted at room temperature.

In the first set of experiments the stability of ICG (instead of cypate which tends to agglomerate on hydrophobic microsome's membrane) (3 mL) was evaluated as described above.

In the next set of experiments fresh solutions of ICG and the NIR dendritic nanoprobes in water (3 mL) were treated in the following order: with NADPH regenerating systems B (10 μL), NADPH regenerating systems A (50 μL), and a solution of rat liver microsomes (5 μL), purchased from BD Biosciences. The injections of the enzymatic mixtures were made directly into the cuvettes after ca. 5 min of initial monitoring.

Fluorescence lifetime was measured using time correlated single photon counting (TCSPC) technique (Horiba) with excitation source NanoLed 773 nm (Horiba), impulse repetition rate 1 MHz at 90° to the detector R928P detector

(Hamamatsu). The detector was set to 820 nm with a 20 nm bandpass. The instrument response function (IRF) was obtained using Rayleigh scatter of Ludox - 40 (Aldrich) (0.03% in MQ water) in a quartz cuvette at 773 nm emission. DAS6 v6.1 decay analysis software (Horiba) was used for lifetime calculations. The fit was judged by χ^2 values and Durbin−Watson parameters and visual observations of fitted line, residuals and autocorrelation function. The lifetime was recorded on 50 ns scale. Total 8200 channels were used with time calibration 6.878525E−03 ns/channel.

$$I(t) = \sum_{i}^{n} \alpha_i \exp(-t/\tau_i) \quad (1)$$

Three-exponential decay equations were used for data fitting. In all cases, lifetime components with insignificant fractional contributions ($f_i < 3\%$) were discarded and decays were considered to be mono- or two-exponential if the sum of fractional contributions (f_1 or $f_1 + f_2$) was higher than 90%. $I(t)$ is intensity as a function of time, τ_i is the decay time of the component i, α_i is the amplitude of the component i at $t = 0$, and n is the number of components equal to 3.

$$f_1 = \alpha_1\tau_1/(\alpha_1\tau_1 + \alpha_2\tau_2) \times 100 f_2 = \alpha_2\tau_2/(\alpha_1\tau_1 + \alpha_2\tau_2) \times 100 \quad (2)$$

f_1 and f_2 are the fractional components (%) with lifetimes τ_1 and τ_2 (ns) with amplitudes α_1 and α_2.

Animal Treatment. All animal procedures were conducted in compliance with Washington University Animal Welfare Committee's requirements for the care and use of laboratory animals in research.

For *in Vivo* Imaging. Mice were anesthetized with ketamine (87 mg/kg) and xylazine (13 mg/kg) via intraperitoneal injection. The nanoprobes (1 mg in PBS) were injected intravenously via lateral tail vein. In vivo mouse images were acquired with a time-domain diffuse optical tomography system (eXplore Optix, GE Healthcare) as reported in the literature. Briefly, the animals were positioned in ventral recumbency on the heated imaging platform. Images were acquired at 15 and 35 min, 1, 5, 8 and 25 h postinjection. The optimal imaging height was assured by side-view CCD camera. The 2D scanning region of interest was selected by top-view CCD. ROIs were raster-scanned for absorption at 780 nm and emission at 830 nm in 3.0 mm increments. Laser power was maintained at 0.04 μW for absorption scans. Laser power for fluorescence imaging was adjusted for optimal signal strength after probe administration.

Acquired images were analyzed with Analysis Workstation software provided by ART. Raw fluorescence data were smoothened by the program utilizing photoinformation from the absorption scan. Fluorescence lifetimes for individual data points were obtained from the temporal point-spread function (TPSF) and used to create a lifetime map by least-squares analysis fitting. The average in vivo fluorescence lifetime was determined for the whole scanning region.

***Ex Vivo* Biodistribution.** Mice injected with the imaging dose of nanoprobes were sacrificed by cervical dislocation under anesthesia at 4 h ($n = 3$), 24 h ($n = 3$) and 8 days ($n = 2$) after injection. Tissue samples from muscle, liver, kidney, spleen, brain, and skin were harvested and placed for fluorescence biodistribution measurement. The relative fluorescence intensities of *ex vivo* organ tissues were plotted in Graphpad Prism. Biodistribution imaging of the treated mice was performed with the Kodak multimodal imaging system (IS4000MM Eastman Kodak Company, New Haven, CT). For fluorescence imaging, broadband illumination from a 150 W halogen lamp was filtered by 755/35 nm optical bandpass filter (Eastman Kodak Company, New Haven, CT) and emission captured via cooled CCD camera after 830 wide-angle long-pass filter (e830WA, Eastman Kodak Company, New Haven, CT). Excitation images were acquired with the same excitation filter, without emission filter for normalization. Fluorescence data were corrected for excitation power by dividing fluorescence images with the corresponding absorption images.

Traumatized Tissue Accumulation. Three 16-week-old male NCR nu/nu mice were anesthetized with ketamine/xylazine cocktail as above. The right carotid artery was exposed through ventral cervical incision, blunt dissection and tissue retraction. For two control mice, the incision was closed with tissue adhesive after artery isolation. Carotid arterial injury was performed in the third mouse by stretching the common carotid artery by insertion of a beaded probe and subsequent ligation of the external carotid. *In vivo* images show high uptake in the surgery site (neck) at 1 and 4 h postinjection.

Acknowledgment. Support from the National Institutes of Health Program of Excellence in Nanotechnology (1 U01 HL080729-01) is acknowledged with thanks. A.A. thanks the University of California Office of the President for a postdoctoral fellowship. The authors acknowledge the assistance of Dr. Cameron Lee (UC Berkeley). We thank Dr. Yunpeng Ye for providing cypate used in this study.

Supporting Information Available: *In vivo* fluorescence intensity map, *in vivo* fluorescence intensity and lifetime maps of cypate−peptide conjugate, fluorescence intensity map post cardiovascular injury, size exclusion chromatograms and dynamic light scattering measurements of NIR dendritic nanoprobes and PEO-polyester dendrimers. This material is available free of charge via the Internet at http://pubs.acs.org.

MP8000952